# Characterization of Cobalt-60 Gamma Ray Emission and Attenuation by Lead

Ryan J. Schlimme[1]

[1]*PHY 353L Modern Laboratory, Department of Physics, The University of Texas at Austin, Austin, TX 78712*

(Dated: February 11, 2024)

We observed spontaneous beta decay of Cobalt-60 to characterize the counting statistics of two distinct energy gamma rays. We counted individual gamma rays using a scintillator/photo-multiplier tube detector. Repeating this process for different durations allowed us to compare counts per time interval and infer an average emission rate. Then, we determined the linear attenuation coefficient of Lead using plates of various thicknesses between the detector and the Cobalt. For the two gamma rays, we calculated emission rates of $145.5 \pm 2.8$ and $108.1 \pm 2.4$ counts/$\mu$s and linear attenuation coefficients of $0.5261 \pm 0.0003$ and $0.4336 \pm 0.0004$ cm$^{-1}$ respectively.

## I. INTRODUCTION

Cobalt-60 ($^{60}$Co) is an unstable isotope with a half-life of 5.27 years [1], which undergoes beta decay — converting a neutron into a proton and releasing an electron — to produce $^{60m}$Ni, as shown in Figure 1. This excited Nickel atom releases its excess energy primarily by emitting two gamma rays (high energy photons) at 1.17 MeV and 1.33 MeV respectively [2]. There is also a small probability of Cobalt-60 decaying into a lower-excitation Nickel, only releasing the 1.33 MeV gamma ray. The $^{60}$Co photon emission spectra is shown in Figure 2.

Radioactive decay is a Poissonian process, one whose probability is characterized by a constant rate over a time interval. In the limit of the rate increasing to infinity, the Poissonian distribution approaches a Gaussian distribution. Since Cobalt emits gamma rays at an approximately constant rate, there is a direct proportionality between time interval length and the counts observed. Therefore, as we increase our time intervals, we expect our data to shift from a Poissonian-modeled to a Gaussian-modeled distribution [5].

Lead (Pb) has widespread use in radiation protection and

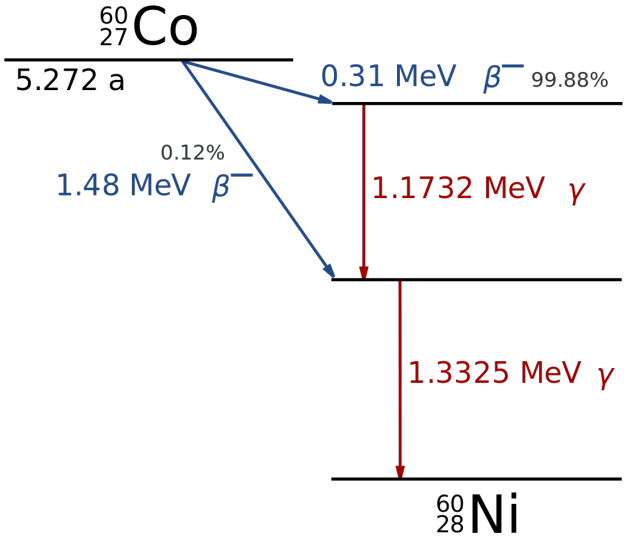


FIG. 1: Illustrating decay process of $^{60}$Co through emission of two $\gamma$-rays at distinct energies [2]

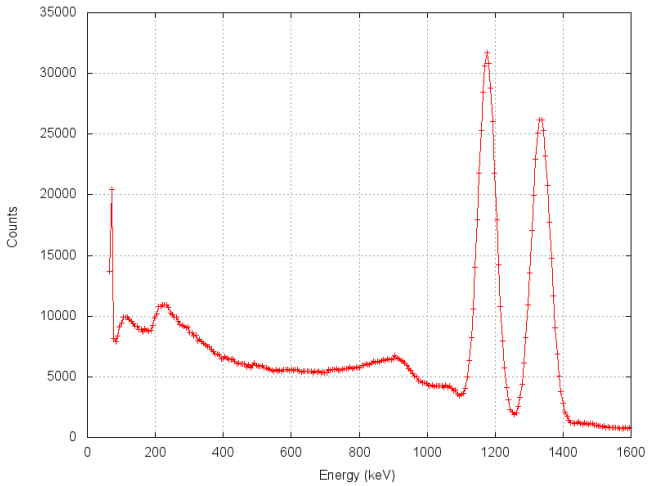


FIG. 2: Spectra of detection energies with low energy counts representing Compton scattering, two high energy peaks representing the two $\gamma$-rays [3, 4]

safety equipment [6]. As an extremely dense element (11.3500 g/cm$^3$) [7], it can attenuate high energy particles, meaning it can absorb or deflect radiation. As the thickness increases, the counts of particles that can pass through the Lead diminishes. This can be modeled by the equation,

$$I(x) = I_0 e^{-\mu x} \tag{1}$$

which describes the intensity, $I$, of radiation per thickness, $x$, as an exponential decay with decay constant, $\mu$, also known as the linear attenuation coefficient [8].

To measure the counting statistics associated with $^{60}$Co decay, we can count the number of gamma ray detections within a short time interval. By repeating the process, we can generate counts which fluctuate according to underlying Poissonian statistics, allowing us to characterize spontaneous emission by averages and standard deviations. We will perform this experiment for different time interval lengths to capture average detections ranging from 2 to 500 counts per interval, allowing us to visualize the differences in distributions attributed to low-average and high-average events.

To measure the linear attenuation coefficient of Lead, we can run the aforementioned process of repeatedly counting

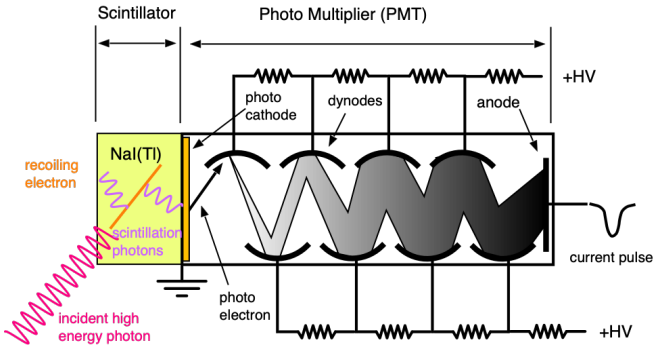


FIG. 3: Schematic of a scintillator and photo-multiplier tube (PMT) [9]

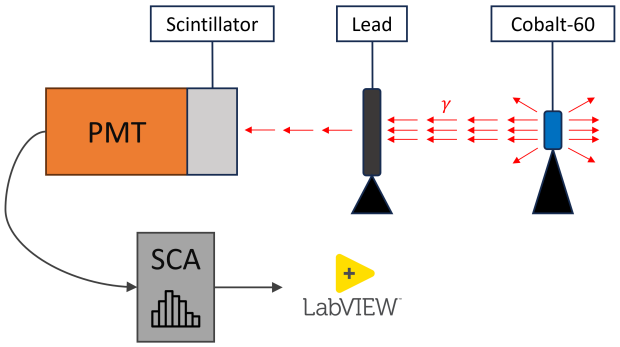


FIG. 4: Experimental setup showing a Cobalt-60 sample irradiating gamma rays in all directions. Those travelling in the direction of the detector are attenuated by the Lead before reaching the scintillator/PMT detector. Electric pulses from the scintillator/PMT are counted by the dual channel SCA and processed using LabView.

emissions per time interval length; however, we will modify our experimental setup, inserting a different thickness Lead plate between the Cobalt source and the detector. We will record the counts as a function of Lead thickness and time interval length. This functional dependence should follow Equation 1.

## II. EXPERIMENTAL SETUP

### A. Apparatus

A common method of detecting individual photons is through the use of a scintillator and photo-multiplier tube (PMT). Scintillators are inorganic crystals or plastics in which a primary electron absorbs an energetic photon, recoiling nearby electrons. Some excited electrons spontaneously decay to their ground states, ejecting photons in all directions. The primary electron, having lost energy to the recoiled electrons, enters the PMT, passing through a photo-cathode, directing it toward a series of dynodes, each of which have a high potential difference placed across them. As the primary electron collides with the dynodes, secondary electrons are released. As the electrons travel through the PMT, the dynodes amplify them until they collide with the anode, resulting in a detectable electrical pulse [3]. A schematic of a scintillator and PMT detection system is shown in Figure 3. We will refer to this system as the detector.

We use two single channel analyzers (SCAs) to communicate the pulses to our analysis software. These devices count all voltages within a set range which are then sent to our computer program for collection and analysis through a National Instruments USB-6361 X Series Data Acquisition Device. To record our data, we use `CountMeIn.vi`, a stable public LabView file which reads the SCA counts, stores them in a text file, and resets the SCA counter to start the next measurement [4].

To ensure we detect only the desired photon energies corresponding to the gamma rays, we calibrate each SCA channel using the following process. We find the gamma rays' corresponding voltage ranges by turning the lower- and upper-boundary knobs until any increase in the upper-boundary and any decrease in the lower-boundary did not significantly change the count. Then, we lowered the upper boundary knob until we approximately halved our output, indicating that we centered on the lower energy gamma ray. We calibrated the second SCA channel in the same manner, except to center on the higher energy gamma ray, we increased the lower boundary knob until we approximately halved our output. Throughout this paper, I will refer to Channel 1 and 2 to refer to the higher- and lower-energy gamma ray measurements.

To determine the linear attenuation coefficient of Lead, we use the same apparatus, but we insert a Lead plate between the Cobalt and the scintillator. This blocks some gamma rays from reaching the detector, lowering the observed counts on average compared to running the experiment without the Lead plate, holding all other parameters constant. A diagram of our experimental setup is shown in Figure 4. Notice that Cobalt-60 emits radiation in all directions. Only radiation travelling toward the detector is counted. With a lead plate between the sample and the detector, some radiation is blocked from reaching the detector.

### B. Data Collection

To estimate the rate of gamma ray emission by Cobalt-60 decay, we count gamma rays over a small time interval. By doing this for several hundred intervals, we generate distributions of counts characterized by a mean and standard deviation. An example of the low mean distributions we observed is shown in Figure 5 whereas an example of the high mean distributions we observed is shown in Figure 6. Repeating this procedure for different time interval lengths allows us to estimate a rate of emission. Additionally, by changing the time interval length, we can visualize the change in the distribution from Poissonian to Gaussian as average counts increase. Notice, the rate of detection depends on the distance from sample to detector as well as the ratio of cross sectional areas of the detector

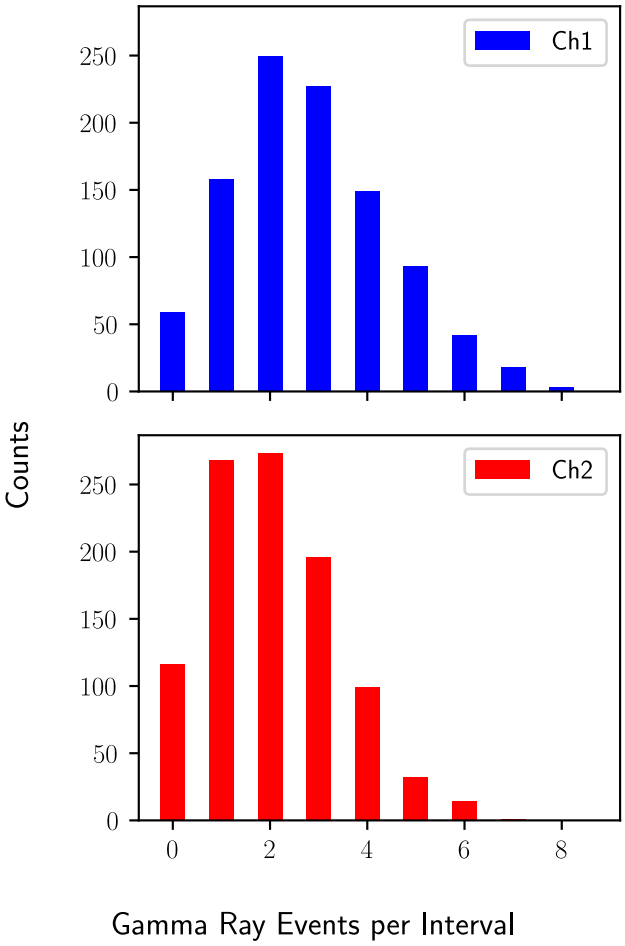


FIG. 5: Raw data from Cobalt-60 decay with time interval length of 25ms, comparing Channels 1 and 2. Notice wider spread and higher average of Channel 1 compared to Channel 2. Both channels show discrete pulse counts with right skew.

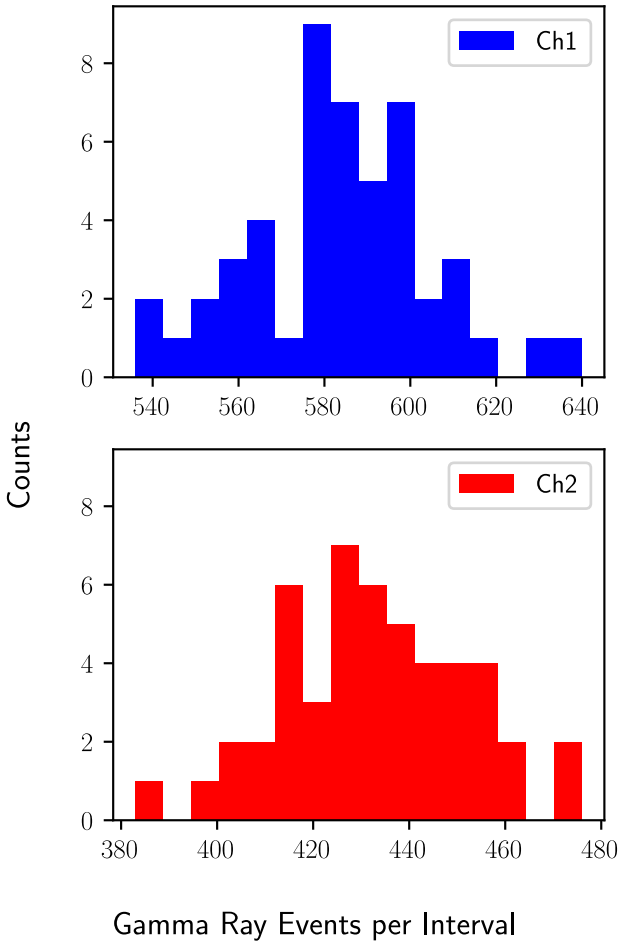


FIG. 6: Raw data from Cobalt-60 decay with time interval length of 4000ms, comparing Channels 1 and 2. Notice higher average of Channel 1 compared to Channel 2. Both channels show approximate normality with similar spread.

and sample. As the distance between the sample and detector increases or as the ratio decreases, the amount of radiation reaching the detector decreases. Therefore, it is important to set these factors constant to isolate the effect of a time interval change on the counting statistics.

To estimate the attenuation coefficient of Lead, we repeat the experiment while inserting various thicknesses of Lead between the Cobalt and the detector. This allows us to determine a functional dependence between Lead thickness and average detection counts while simultaneously verifying the count decay rate. Upon analyzing the data, we found this test unnecessary. Instead, we recommend repeatedly counting detections over a the same fixed time interval length for each Lead plate.

### C. Data Analysis

When analyzing the Cobalt decay histograms, we plotted the average counts vs the time interval lengths and observed a roughly linear relationship shown in Figure 7. Therefore, there is a constant rate of gamma ray emission characterized by the slope of the line we fit to our data. Theoretically, we expect a vertical intercept of 0; however, it is impossible to perform the experiment with a time interval length of 0, so accurately determining the intercept is difficult.

Using `scipy.optimize.curve_fit` — a Python function to fit data to a theoretical function using least squares regression — we fit a linear function $C(t) = rt + C_o$ for the counts as a function of time interval length (in ms), $C(t)$, in terms of the rate of decay, $r$, and the counts for time interval of 0, $C_0$. We included the latter term to improve the fit of the model, but data in accordance with theory should have this parameter tend toward 0. Our fit determined $r = 145.5 \pm 2.8$ counts/$\mu$s and $r = 108.1 \pm 2.4$ counts/$\mu$s with intercept $(5.3 \pm 0.03) \times 10^{-2}$

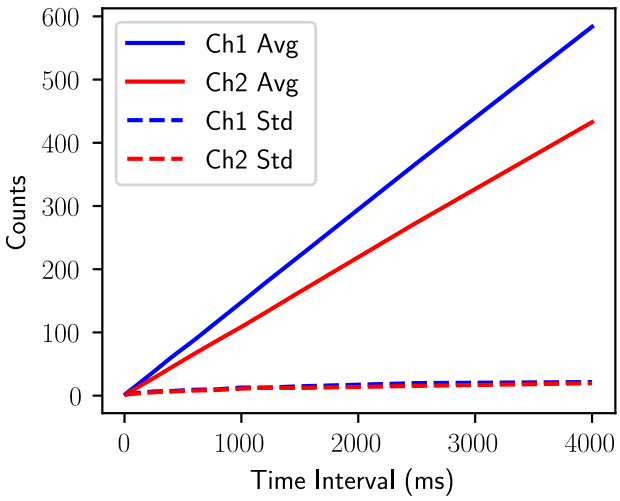


FIG. 7: Illustrating the linear relationship between average counts and time length interval, blue symbolizing Channel 1 and red symbolizing Channel 2. Solid lines indicate average count values where dashed lines indicate the corresponding standard deviations.

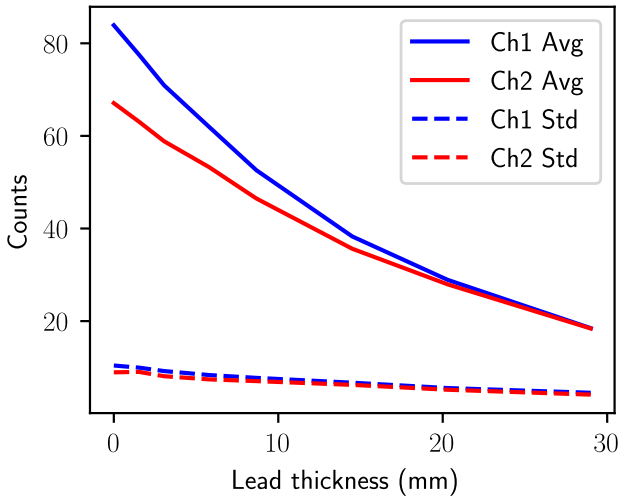


FIG. 8: Illustrating the attenuation of $^{60}$Co by Lead, blue symbolizing Channel 1 and red symbolizing Channel 2. Solid lines indicate average count values where dashed lines indicate the corresponding standard deviations.

and $(4.3 \pm 0.04) \times 10^{-2}$ for the first and second SCA channels respectively. Parameter uncertainty was found by calculating the fitting error using `scipy`.

To determine the linear attenuation coefficient of Lead, we calculated the average and standard deviation of counts for each trial. For each time interval length, we determined the average counts for each Lead plate. Then, we plotted the average and standard deviation of counts as a function Lead thickness faceted by the time interval length. We observed an exponential decay; however, we were not able to measure an average count close to 0 as we did not have a sufficiently thick Lead plate. An example of one of these plots is shown in Figure 8.

Using `scipy.optimize.curve_fit`, we fit an exponential function $C(x) = C_0 e^{-\mu x}$ for the counts, $C(x)$, as a function of Lead thickness, $x$, in cm, and the linear attenuation coefficient, $\mu$, in cm$^{-1}$. Using the model fit, we generated parameters for each of the time interval lengths. Comparing the outputs, we noticed the value of $\mu$ among time interval lengths were very similar. Therefore, to determine the overall linear attenuation coefficient, we averaged the linear attenuation coefficient parameters. To calculate our uncertainty, we averaged the variance of the parameter fit and then computed the square root to determine the standard deviation of the averaged error. We calculated linear attenuation coefficients of $0.5261 \pm 0.0003$ and $0.4336 \pm 0.0004$ for the two gamma rays respectively.

## III. DISCUSSION

We determined Cobalt-60 gamma ray emission rates of $r = 145.5 \pm 2.8$ counts/$\mu$s and $r = 108.1 \pm 2.4$ counts/$\mu$s respectively. One can estimate the theoretical counting rate of Cobalt-60 gamma ray emissions should they know the mass and age of the Cobalt-60 sample. Using the half life and age of our sample, we can estimate the total mass of Cobalt-60 present. Then, we can use the ratio of cross sectional areas to estimate the proportion of total radiation we can detect, extrapolating our results to determine the total emission rate by multiplying our results by the ratio of total spherical surface area to the cross sectional area of our detector. Unfortunately, we could not measure the age or mass of our sample, and therefore cannot make an estimate. However, we found the emission distribution as approximately Gaussian for large averages and Poissonian for small averages in accordance with theory that radioactive decay is a random process.

We found the linear attenuation coefficient of Lead as $0.5261 \pm 0.0003$ and $0.4336 \pm 0.0004$ cm$^{-1}$ for the two gamma rays. The current accepted linear attenuation coefficient of Lead for 1.25 MeV photons (the average energy of the two gamma rays), accounting for the build up factor — a correction to include scattered photons which are not detected [10] — is 0.5127 cm$^{-1}$ [8, 11]. Our results approximately agree with theory.

There could have been minor discrepancies with the effective thickness of Lead induced by a slight tilt in the plate. If the Lead plates are not perpendicular with the axis of the detector (the axis at which the gamma rays travel from the Cobalt to the scintillator), the effective thickness of Lead would be slightly greater than anticipated, causing the calculated attenuation coefficient to be higher than theory would suggest. Additionally, if we miscalibrated our SCA voltage limits to include lower- or higher- energy photons, our attenuation coefficient would consequently be greater or lower than theory suggests. The attenuation coefficient is inversely proportional to the energy of the photon as higher energy particles have sufficient energy to pass through materials.

## IV. CONCLUSIONS

We found the average gamma ray emission rate of the Cobalt-60 decay using a scintillator and PMT, allowing us to qualify individual photons as opposed to total deposited energy, the more standard measurement for measuring radioactive emission. By repeatedly measuring the counted photons per time interval, we quantified the mean and standard deviation of the gamma ray emission. By repeating the experiment for many different time interval lengths, we estimated an emission rate using a linear model fit. We were not able to compare our results to theory as we did not know the sample mass or age, but we confirmed our data to agree with the theory of radioactive decay as a random process by interpreting the shape of count distributions.

We determined the linear attenuation coefficient of Lead by inserting Lead plates between our sample and our detector. By testing the dependence of observed count statistics on the thickness of Lead, we found an exponential decay of counts relative to Lead thickness, holding time interval length constant. This agreed with current models of attenuation, so we modeled our data with an exponential decay function, finding parameters for the linear attenuation coefficient which agreed with modern estimates, accounting for theoretical corrections.

I would like to thank my lab partner, Adrian, for his invaluable assistance during the experiment. Additionally, I would like to thank Dr Greg Sitz for assisting our efforts in and outside of the lab. I would also like to thank the creators of Python, Pandas, Numpy, Scipy, Matplotlib, and PowerPoint who helped make possible the analysis and figures in this paper. This paper was written and compiled in LaTeX using the Overleaf online editor.

[1] E. D. Collins and C. L. Ottinger, in *Encyclopedia of Physical Science and Technology*, edited by R. A. Meyers (Academic Press, New York, 2003) 3rd ed., pp. 109–126.
[2] J. Yang, G. Koller, C. Fares, F. Ren, S. Pearton, J. Bae, J. Kim, and D. Smith, ECS Journal of Solid State Science and Technology **8**, Q3041 (2019).
[3] G. O. Sitz (2024), background knowledge on Cobalt-60 decay basics, scintillator and photomultiplier tube design.
[4] G. O. Sitz, PHY 353L: Modern Lab, `https://web2.ph.utexas.edu/~phy353l/RadioactiveDecay/RadioactiveDecay.html` (2024), Accessed: 09 February 2024.
[5] A. C. Melissinos and J. Napolitano (1966).
[6] G. L. Stukenbroeker, C. F. Bonilla, and R. W. Peterson, Nuclear Engineering and Design **13**, 3 (1970).
[7] National Institute of Standards and Technology, Composition of Lead, `https://physics.nist.gov/cgi-bin/Star/compos.pl?mode=text&matno=082` (2017), Accessed: 05 February 2024.
[8] R. E. F. Arthur P Chilton, J Kenneth Shultis, *Principles of Radiation Shielding* (Prentice-Hall, 1984).
[9] W. U. Boeglin, Modern lab manual: Scintillation detector, `https://wanda.fiu.edu/boeglinw/courses/Modern_lab_manual3/scintillator.html` (2024), Accessed: 05 February 2024.
[10] Y. Harima, Radiation Physics and Chemistry **41**, 631 (1993).
[11] R. E. F. J Kenneth Shultis, *Radiation Shielding* (American Nuclear Society, 2000).